Available online at www.sciencedirect.com
SCIENCE DIRECT®
Catalysis Today 96 (2004) 251–257
CATALYSIS TODAY
www.elsevier.com/locate/cattod

Structure–activity relationships in alumina-supported molybdena–vanadia catalysts for propane oxidative dehydrogenation

Miguel A. Bañares*, Sheima J. Khatib

Instituto de Catálisis y Petroleoquímica, CSIC, Marie Curie 2, E-28049-Madrid, Spain

Available online 24 August 2004

Abstract

The interactions between Mo and V on alumina are studied for the oxidative dehydrogenation (ODH) of propane. Dispersed surface molybdena and vanadia species share alumina support but show no interaction below Mo + V monolayer coverage. Vanadia and molybdena species react on alumina into mixed Mo–V–(Al)–O above Mo + V monolayer coverage, which nature depends on environmental conditions. Molybdena sites may form $Al_2(MoO_4)_3$ or Mo–V–O phases depending on loading and temperature. The Mo–V–O phases spread on the support as separate surface oxides at lower coverage, such trend appears promoted by ODH reaction conditions.
© 2004 Elsevier B.V. All rights reserved.

Keywords: Operando; Raman; Vanadia; Molybdena; Mixed oxides; Propane; ODH; Structure–activity relationships

1. Introduction

The oxidative dehydrogenation (ODH) represents a promising emerging technology being investigated to convert light alkane feeds to their respective valuable olefin counterparts. Compared to non-oxidative dehydrogenation (DH), ODH routes render the process to be exothermic due to the use of an oxidant, and thus, thermodynamically favorable. This has significant economic advantages over the conventional DH processes, which are endothermic, with respect to energy cost to operate the process and capital requirements. In addition, the reaction temperature is lower than conventional DH reactions, and therefore, the life of the catalyst is prolonged. Furthermore, deactivation problems due to coke formation are prevented and the thermal cracking of heavier alkanes is minimized, but non-selective CO_x formation must be considered in the development of ODH processes. Most catalysts for selective oxidation possess vanadium as a key element [1–8]. Mixed-metal oxide catalysts are efficient for alkane oxidation to olefins, oxygenates and nitriles [2–8] and their performance can be tuned by a third component [1–7]. Thus, it is important to understand the structure–activity relationships in mixed Mo–V oxides. The nature of the active phase in bulk mixed-metal oxide catalysts is not easy to assess. Some *operando* Raman-GC studies show a close correlation between the oxidation state of Mo sites and the selectivity [9]. While the exact nature of the surface in mixed-metal oxides is not clear, it has to be related to the bulk structure. The reaction environment affects the surface and bulk structures. By changing, Mo + V loading, it is possible to possess dispersed Mo and dispersed V oxide species on alumina, and three-dimensional Mo oxides, V oxides and mixed Mo–V oxides.

2. Experimental

2.1. Preparation of samples

Alumina-supported Mo–V catalysts were prepared with different Mo + V loadings and at a constant Mo/V = 1 atomic ratio. Mo and V were co-impregnated by a solution of VO_3NH_4 + $Mo_7O_{24}(NH_4)_6{\cdot}4H_2O$ and dried in a rotatory

* Corresponding author. Tel.: +34 91 585 4788; fax: +34 91 585 4760.
E-mail address: mbanares@icp.csic.es (M.A. Bañares).

0920-5861/$ – see front matter © 2004 Elsevier B.V. All rights reserved.
doi:10.1016/j.cattod.2004.06.152

evaporator at 80 °C. The resulting solid was dried at 120 °C for 1 h and then calcined at 450 °C for 5 h. The catalysts are named as *x*MoVAl, or *x*MoAl or *x*VAl, where *x* indicates the number of (Mo + V) monolayer. We have assumed a total number of 9 atoms/nm^2 of alumina support as a monolayer value [10].

2.2. Activity measurements

Activity measurements were performed using a conventional microreactor with on-line gas chromatograph equipped with a thermal conductivity detector. The correctness of the analytical determinations was checked for each test by verification that the carbon balance (based on the propane converted) was within the cumulative mean error of the determinations (±10%). To prevent participation of homogeneous reactivity the reactor was designed to minimize gas-phase activation of propane. Tests were made using 0.3 g of sample with particle dimensions in the 0.25–0.125 mm range. Tests were made using the following feedstock: 57% O_2 and 5% propane in helium. The total flow rate was 90 ml/min. Yields and selectivities in products were determined on the basis of the moles of propane feed and products, considering the number of carbon atoms in each molecule.

2.3. Operando Raman spectroscopy

Operando Raman spectra were run with a single monochromator Renishaw System 1000 equipped with a cooled CCD detector (−73 °C) and holographic super-Notch filter. The holographic Notch filter removes the elastic scattering while the Raman signal remains high. The samples were excited with the 514 nm Ar line; spectral resolution was ca. 3 cm^{-1}. The spectra were obtained under reaction conditions (ca. 480 °C) in a home-made fixed-bed *operando* reaction cell, with optical quality quartz walls. The activity in the *operando* reaction cell was measured with an on-line gas chromatograph equipped with a thermal conductivity detector (Hewlett-Packard 5890-Series II). The correctness of the analytical determinations was checked for each test by verification that the carbon balance (based on the propane converted) was within the cumulative mean error of the determinations (±10%). To prevent participation of homogeneous reactivity the reactor was designed to minimize gas-phase activation of propane. The tests were made using 0.3 g of sample with particle dimensions in the 0.25–0.125 mm range. Yields and selectivities in products were determined on the basis of the moles of propane feed and products, considering the number of carbon atoms in each molecule. The activity values did not differentiate significantly from those obtained in a conventional fixed-bed reactor.

3. Results

Fig. 1 shows the Raman spectra of dehydrated 0.5VAl, 0.5MoAl and *x*MoVAl catalysts. 0.5MoAl exhibits a Raman band at 996 cm^{-1}, characteristic of the Mo=O stretching mode of surface monooxo molybdenum oxide species [11]. 0.5VAl catalyst exhibits the Raman bands of surface vanadium oxide species at 1031 cm^{-1} (V=O stretching mode) and a broad feature centered at 850 cm^{-1} (V–O–V stretching mode) [11]. The Raman bands of surface Mo and surface V

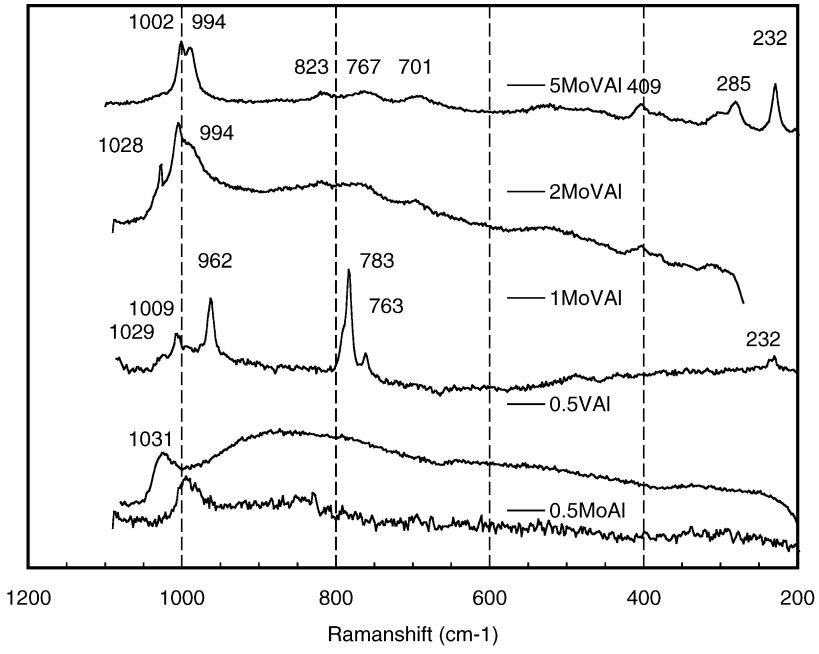

Fig. 1. Raman spectra of dehydrated 0.5MoAl, 0.5VAl, 1MoVAl, 2MoVAl and 5MoVAl fresh catalysts.

oxide species are sensitive to hydration. The fresh dehydrated molybdena–vanadia catalysts, 1MoVAl, 2MoVAl and 5MoVAl exhibit different Raman bands, depending on Mo + V coverage on alumina. At ca. one Mo + V monolayer, the Raman spectrum looks different and new Raman bands appear at 962, 783 and 763 cm^{-1}. These bands are not those of alpha-MoO_3 (999, 820, 672, 383, 342, 290, 250, 163 cm^{-1}) or V_2O_5 (994, 701, 525, 409, 295, 285, and 143 cm^{-1}). The relative intensity and position of the Raman bands at 965 and 786 cm^{-1} resemble those of alpha-MoO_3 shifted by ca. 30 cm^{-1}, this may be indicative of a distorted MoO_3 lattice due to some V cations [12], such interaction has been proposed elsewhere [13]. The Raman band at 763 cm^{-1} may correspond to the mixed Mo–V–O phase reported by Bell and coworkers [14]. There are several known Mo–V–O phases [15–26]; however, at this moment, these Raman bands are not assigned and XRD patterns are very weak; thus, we name it phase-I. These Raman bands do not appear to correspond to reduced Mo oxide species, which exhibit Raman bands in the 800–950 cm^{-1} region [27–29]. Thus, it appears that Mo and V interact forming mixed Mo–V–O phases above monolayer coverage, this is interesting since those phases appear to be efficient for alkane activation [2–7]. 2MoVAl and 5MoVAl exhibit weak features near 994, 701, 525, 409, 295 and 285 cm^{-1}, which indicates the presence of trace amounts of V_2O_5. The intense Raman bands at 1028, 1005 and the weak feature at 381 cm^{-1} in 2MoVAl are not sensitive to hydration and correspond in position and relative intensity to those of $Al_2(MoO_4)_3$ [30–33]; which is not present in the fresh 5MoVAl. The Raman features near 767 and 232 cm^{-1} may suggest the presence of the Mo–V–O phase-I in 2MoVAl; this phase is more evident for 5MoVAl.

Fig. 2 shows the conversion of propane versus the reaction temperature for 0.5VAl, 0.5MoAl and *x*MoVAl catalysts. As expected, the vanadia catalyst is at least an order of magnitude more active than the molybdena catalyst. The activity of 1MoVAl and 2MoVAl catalysts is essentially the same than that of 0.5VAl; but the reaction becomes unstable above 340 °C due to hot spots for 2MoVAl. Thus, several samples of 2MoVAl were run up to 340 °C and others above such temperature. Both catalysts were characterized after reaction. Those run below 340 °C are identified by the suffix—LT (after lower temperatures); and those run at temperatures above 340 °C are identified by the suffix—HT (after higher temperatures). 5MoVAl exhibits lower activity than 1MoVAl and 2MoVAl.

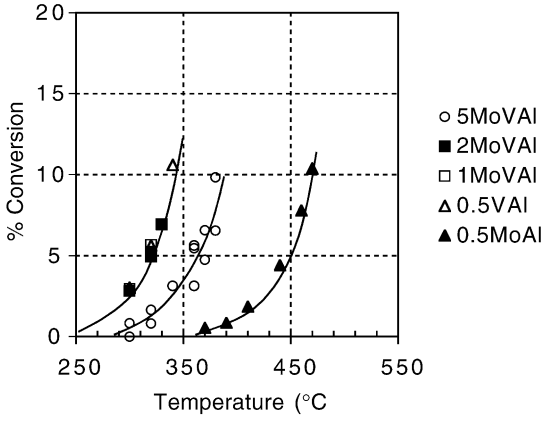

Fig. 2. Propane ODH conversion on 0.5MoAl, 0.5VAl, 1MoVAl, 2MoVAl and 5MoVAl. Reaction condition: catalyst weight, 200 mg; total flow, 90 ml/min; reaction feed: $O_2/C_3H_8/He$ = 1/12/8 molar.

The propylene selectivity–conversion profiles (Fig. 3) show three groups of catalysts. 0.5MoAl exhibits the highest selectivity, but it is much less active. 0.5VAl and 1MoVAl exhibit higher selectivity to propylene than 2MoVAl and 5MoVAl, which are the least selective. This trend reverses for carbon monoxide. The differences in CO_2 selectivity are much lower and 0.5VAl and 0.5MoVAl exhibit a slightly higher selectivity to CO_2. It is interesting to compare 0.5VAl and 1MoVAl since both possess the same vanadia loading but different structures. However, both catalysts exhibit the same activity and selectivity. This is rather surprising, since mixed Mo–V–O phases typically exhibit high activity and selectivity for alkane oxidation [2–8]. The Raman spectra of the used catalysts may provide some additional information.

There is no appreciable change in the Raman spectrum of used 0.5VAl, in line with many studies of alumina-supported vanadia during the oxidation of ethane [34,35], propane [36] and butane [35,37]. Used 0.5MoAl shows no change either. These spectra are not presented. Fig. 4 illustrates the Raman spectra of dehydrated used *x*MoVAl catalysts. Used 1MoVAl exhibits a completely different Raman spectrum; hydration-sensitive Raman bands near 1029 and 1006 cm^{-1} evidence the V=O and Mo=O stretching modes of surface vanadia and surface molybdena species. The broad Raman band near 860 cm^{-1} is indicative of the stretching mode of bridging oxygens in surface polymeric vanadia and molybdena species. Used 2MoVAl-LT and used 5MoVAl exhibit Raman bands at 1037 and 1002 cm^{-1}, not sensitive to hydration, which correspond to $Al_2(MoO_4)_3$. Used 5MoVAl exhibits the diffraction pattern of $Al_2(MoO_4)_3$ (not shown), which was not present in the fresh 5MoVAl. Used 2MoVAl-HT exhibits a significantly different Raman spectrum; no Raman bands are evident above 900 cm^{-1}. Raman bands near 900 and 700 cm^{-1} have been assigned to partially reduced molybdates, possessing Magnéli-type MoO_{3-x} phases [28,29], which stabilize oxygen defects in binary Mo–V oxides [38–40]. The assignment of Raman bands in Mo–V–O system is not clear in literature yet; however, they do not appear to belong to $Mo_4V_6O_{25}$, which exhibits Raman bands at 917, 860 and 840 cm^{-1} [41]. The chemistry of the Mo–V–Al–O system presents more possibilities than the Mo–V–O system; phases like $AlVMoO_7$, $Mo_6V_9O_{40}$, $Al_2(MoO_4)_3$ may interconvert at 590 °C and above [42–44]. Such temperatures may be reached during reaction at the hot spots at high temperature in 2MoVAl-HT. $Al_2(MoO_4)_3$ is present in used 5MoVAl but it is no longer present in 2MoVAl after reaction. $Al_2(MoO_4)_3$—present in fresh 2MoVAl—reacts at

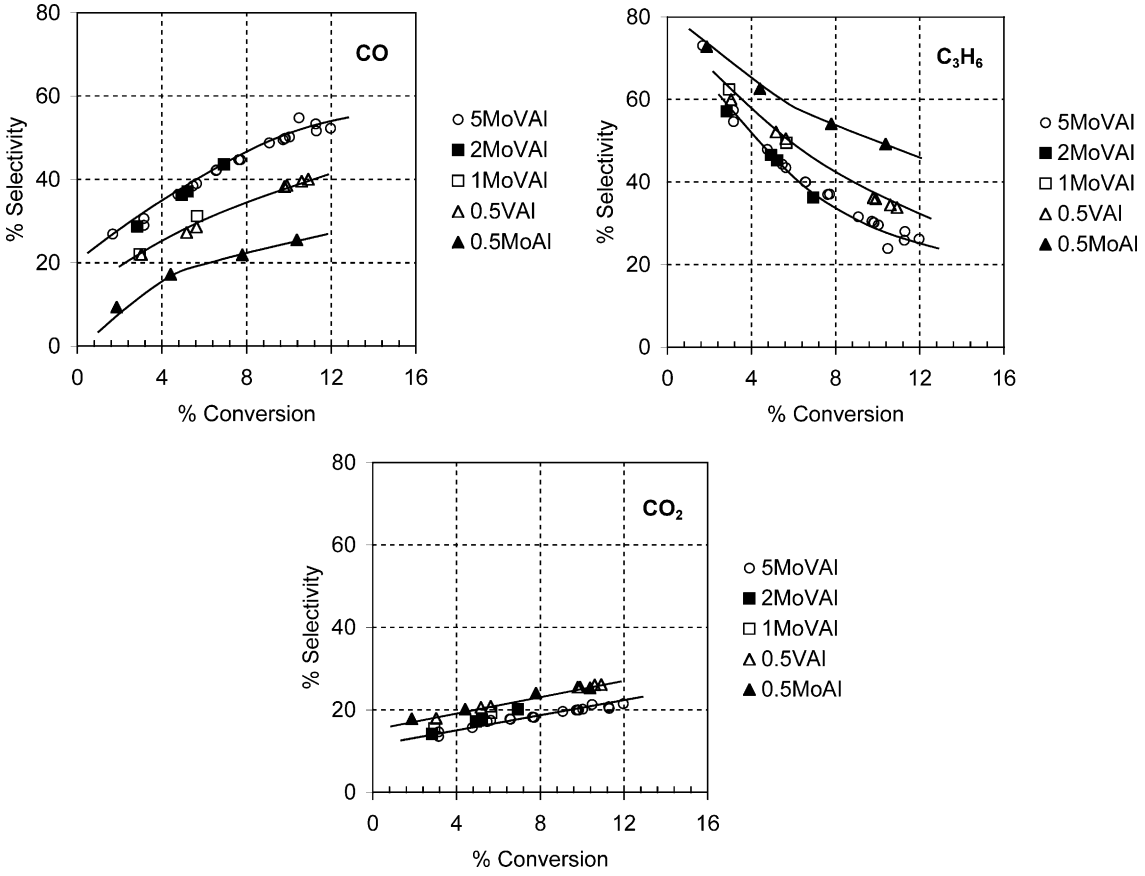

Fig. 3. Selectivity conversion profiles for 0.5MoAl, 0.5VAl, 1MoVAl, 2MoVAl and 5MoVAl. Reaction condition: catalyst weight, 200 mg; total flow, 90 ml/min; reaction feed: O_2/C_3H_8/He = 1/12/8 molar.

high temperatures in air with vanadia into $Mo_6V_9O_{40}$ [44], which possesses some reduced sites [44,45]. Thus, the Raman bands at 862, 798 and 700 cm^{-1} are consistent with the presence of some reduced Mo–V–O phase, possibly $Mo_6V_9O_{40}$. However, this assignment need further validation and XRD patters are not conclusive, probably due to the

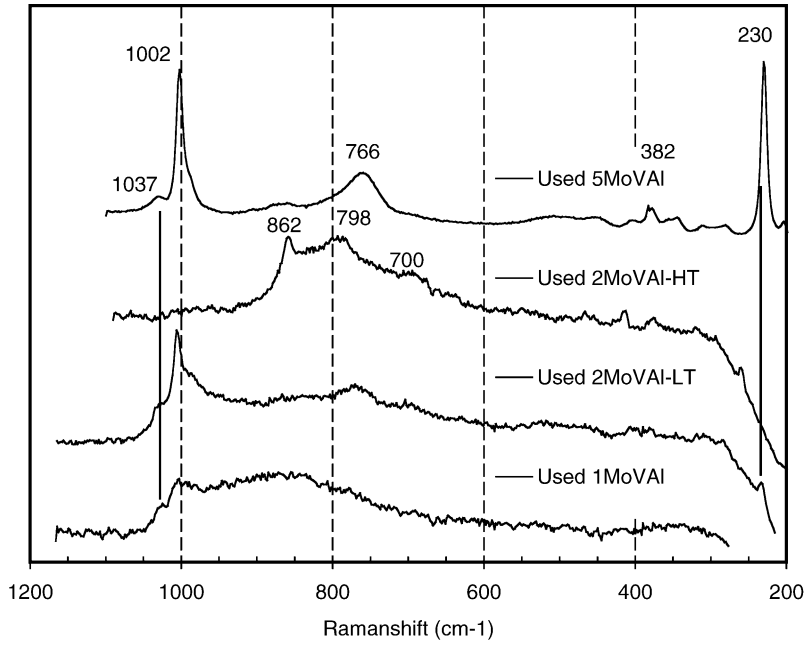

Fig. 4. Raman spectra of dehydrated 0.5MoAl, 0.5VAl, 1MoVAl, 2MoVAl and 5MoVAl used catalysts.

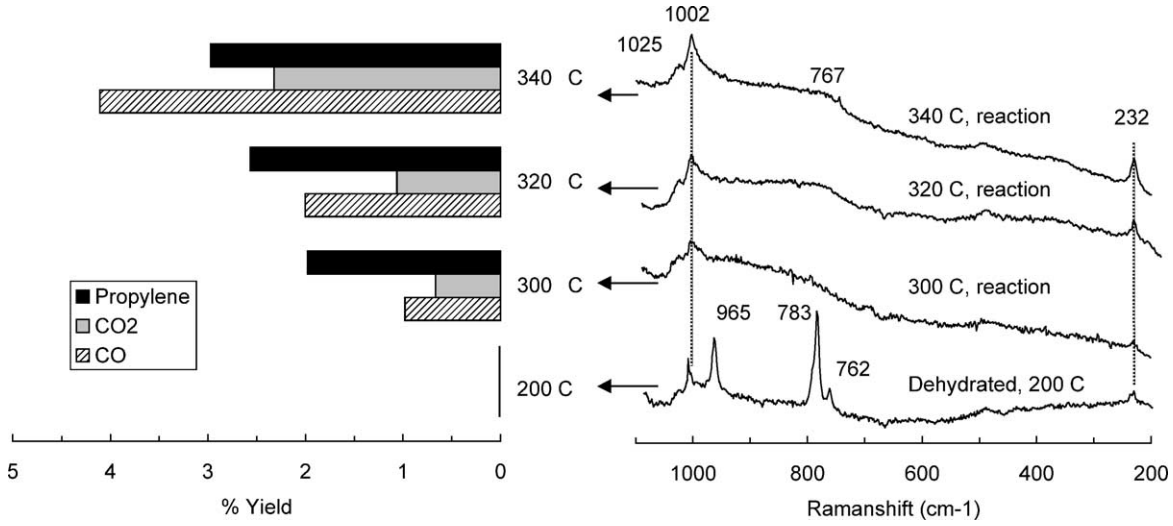

Fig. 5. *Operando* Raman-GC study of catalyst 1MoVAl during propane ODH reaction. Left panel, conversion to the different products during Raman spectra acquisition; right panel, simultaneous Raman spectra. Reaction conditions like in Fig. 2.

small size of the aggregates; therefore, we name it as phase-II, which should be more reduced than phase-I.

The lack of differences in catalytic activity between 0.5VAl and 1MoVAl catalyst appears due to the breakdown of mixed Mo–V–O phases into surface molybdena and surface vanadia phases (Fig. 4). It is interesting to determine which is the actual status of the Mo and V phases during propane oxidative dehydrogenation. To do so, we have run reaction in situ Raman studies with simultaneous on-line GC activity/selectivity measurements in a cell designed as a catalytic reactor, free of gas-phase reaction interference. The reaction feed flows through the powdered catalyst bed. The catalyst particle size and the residence conditions have been selected to prevent diffusion control. The above-mentioned constrains for a reaction in situ study combined with simultaneous activity measurement constitute the so-called *operando* study of the system (*operando* Raman-GC study, in this case) [11,36,46–48]. Fig. 5 shows the *operando* Raman-GC study of 1MoVAl catalyst during propane oxidative dehydrogenation. The right panel illustrates the Raman spectra, taken at the indicated temperature during catalytic operation. The left panel illustrates the corresponding activity data (yield values) obtained simultaneously to the Raman spectra during reaction. Table 1 compares the activity data at 320 °C for 1MoVAl in the conventional fixed-bed reactor and in the *operando* fixed-bed reaction cell. The consistency between the activity/selectivity data in the conventional fixed-bed reactor and in the *operando* fixed-bed reaction cell is critical for a reliable *operando* study.

Table 1
Catalytic activity of 1MoVAl in the conventional and *operando* fixed-bed reactors

Reactor	Temperature (°C)	Conversion (mol.%)	Selectivity		
			Propylene	CO	CO_2
Conventional	320	5.7	49.5	31.2	19.3
Operando	320	5.6	45.6	35.6	18.8

Reaction conditions: catalyst weight 300 mg; total flow 90 ml/min; C_3H_8/O_2/He = 1/12/8 molar.

The *operando* Raman-GC study of 1MoVAl during the oxidative dehydrogenation of propane shows the transformation of the Mo–V–O phases (Fig. 5). The Raman bands of the mixed Mo–V–O and of the V-distorted MoO_3 phases are present in the fresh dehydrated catalyst. The molecular structures of the Mo and V phases change as soon as the system affords some conversion of propane (ca. 2%). The Raman bands of Mo–V–O phases are replaced by new Raman bands at 1025 and 1002 cm^{-1}, characteristic of the V=O and Mo=O stretching modes of surface vanadia and molybdena species, respectively. The stretching mode of bridging oxygen sites of surface polymeric vanadia and molybdena show broad Raman bands at 800–900 cm^{-1}. The feature near 770 cm^{-1} is close to that recorded at 762 cm^{-1} [14] but it possesses very low intensity and a very broad shape. This feature could be indicative of an ill-defined Mo–V–O phase-I; however, the Raman spectra suggest that most of the Mo and V species have spread as surface molybdena and vanadia on alumina. Therefore, no Mo–V–O phase appears predominant during propane oxidative dehydrogenation at Mo + V coverage near monolayer. Thus, the performance of 1MoVAl is not due to Mo–V–O phase-I but to surface molybdena and surface vanadia species.

4. Discussion

The structures of molybdena and vanadia on alumina depend on the total Mo + V coverage on alumina and on the reactive environment, which determine the interactions between Mo, V and Al. So, two distinct scenarios result if total Mo + V coverage is below or above its dispersion limit

on alumina (monolayer). An interesting borderline situation occurs near the dispersion limit loading of Mo + V on alumina (near monolayer coverage).

4.1. Below the Mo + V monolayer coverage on alumina

When Mo and V are supported on alumina, their structures depend on the total Mo + V coverage on alumina and on the reaction conditions. Below monolayer coverage, they disperse on alumina, and no apparent interaction takes place among the different cations. This scenario has already been described, the coexistence of two ''non-interacting'' oxides does not afford a new phase and they share the surface, leading to a ''crowding'' effect [49,50]. This preference for spreading is in line with the more favorable situation of oxides being as a dispersed layer rather than as three-dimensional aggregates on top of the support [51,52].

4.2. Above the Mo + V monolayer coverage on alumina

For a single oxide, three-dimensional structures develop at monolayer coverage and above. Consequently, a new scenario appears when Mo + V loading is above monolayer coverage: both Mo and V aggregate. This may afford Mo–V interactions, since there are many mixed Mo–V oxides [5,14–26]. Upon calcination, it appears that the interaction is moderate, a V-modified MoO_3 (Raman bands at 962, 783 cm^{-1}) is the predominant Mo–V–O phase. Such phase appears to be α-MoO_3 with some minor amounts of vanadium. Some mixed Mo–V–O phases possess very low V/Mo ratios [13], like 0.49 [25] and 0.07 [26]. The presence of a mixed Mo–V–O phase-I (Raman band at 766 cm^{-1}) becomes increasingly important in the used catalysts. It is likely that phase-I possesses a higher V/Mo ratio than the V-modified MoO_3, so that phase-I evidences a more extensive entanglement of Mo and V ions. Such interaction is evident in the used catalysts since lattice oxygen mobility during the catalytic redox cycle promotes the interaction between Mo and V. Many of the described Mo–V–O phases exhibit some reduction of the Mo or V sites [15–17,19,21–26,28,29,45]. The Raman bands of phase-II (862, 798, 700 cm^{-1}) are not assigned yet, but Raman bands between 860 and 700 cm^{-1} are characteristic of partially reduced molybdates [28,29]. As commented in the Section 3, the Mo–V–O phase-II should be more reduced than Mo–V–O phase-I. Operation under ODH operation conditions affords phase-I; which is observed in used 5MoVAl and 2MoVAl-LT. During catalytic operation with hot spots, the resulting mixed Mo–V–O phase (phase-II) appears oxygen defective (perhaps $Mo_6V_9O_{40}$). Several driving forces may compete in shaping supported mixed oxides in the reaction environment. A reducing environment tends to aggregate supported oxides [53,54], and may promote the formation of mixed Mo–V oxides, which stabilize partially reduced sites. Reaction conditions aggregate [54] and disperses [55] supported oxides, due to oxide ion mobility. The interaction with water, generated during reaction, may also affect the dispersion states and structure, as reported elsewhere [56]. Water may also coordinate to Mo species to form volatile oxo-hydroxides. There is a wide panorama of possible combinations in the Mo–V–Al system [42–44]. The formation of $Al_2(MoO_4)_3$ (Raman bands at 1028, 1002 and 382 cm^{-1}) could be promoted by molybdena loading. Such phase is stable in the presence of vanadia up to 590 °C [44]. These factors are under a detailed study now.

4.3. Near the Mo + V monolayer coverage on alumina

A borderline situation may occur near Mo + V monolayer coverage. Mo–V–O phases may form during catalyst preparation near monolayer coverage (1MoVAl). At this loading, it is unlikely to form $Al_2(MoO_4)_3$ with our reaction conditions; thus, most interactions affect preferentially vanadia and molybdena species. The reaction conditions promote lattice oxygen mobility, which may break and spread mixed Mo–V–O phases into the separate surface oxides. Such oxygen mobility enables the entanglement of Mo and V cations above Mo + V monolayer coverage. However, near monolayer coverage, such trend competes with spreading, which is energetically favored [51,52]; thus spreading into the corresponding surface oxides. A similar effect has also been observed for mixed V–Sb–O phases on alumina during propane ammoxidation reaction [57]: $VSbO_4$ forms near the monolayer coverage, but it spreads during ammoxidation reaction. Here, surface Mo and V share the alumina support, contributing to the reaction with their own reactivity and no significant cooperation appears to take place for propane ODH. The total loading of Mo and V is half a monolayer for each of them and the propane ODH activity of surface Mo species is an order of magnitude lower than that of surface V species. Thus, the contribution of Mo species to the activity of the V species in 1MoVAl is hardly appreciable. This accounts for the very similar performances of 1MoVAl and 0.5VAl, which possess the same vanadia loading and vanadia structure during reaction.

5. Conclusions

The total Mo + V coverage and the reaction conditions determine the resulting phases on alumina-supported mixed Mo–V oxides. The stability of Mo–V–(Al)–O phases depends on the Mo + V coverage and on the reaction environment, due to oxygen mobility during redox cycles. Mo–V–Al–O phases form on alumina support above the Mo + V monolayer coverage. Above Mo + V monolayer coverage, reducing reaction environments afford reduced Mo–V–O phases. At high molybdena loading, Mo–V–O phases compete with the formation of aluminum molybdate, which breaks in the presence of vanadia at elevated temperatures forming, probably, $Mo_6V_9O_{40}$. Below Mo + V monolayer coverage, bulk Mo–V–O phases spread during reaction.

Thus, Mo and V share the alumina support and contribute to the reaction with their own reactivity. No significant cooperation between dispersed V and dispersed Mo oxides appear to take place for propane ODH. Vanadium dominates the performance, since the activity per vanadium site is nearly 10 times than that of the molybdenum sites in supported oxides.

Acknowledgements

This research was funded by MCyT (Spain) project MAT-2002-0400-C02-01. Grant IN96-0053 partially funded the acquisition of the Raman system. SJK thanks CSIC-EU for an ''I3P'' doctorate studies fellowship. The authors thank the support of Mr. Ramón Tomé Neches and Mr. Francisco Izquierdo Galve for the fabrication of the *operando* cell at the Institute of Catalysis and Petrochemistry, CSIC, in Madrid.

References

[1] R.K. Grasselli, Catal. Today 49 (1999) 141.
[2] T. Blasco, J.M. López-Nieto, Appl. Catal. A 157 (1997) 117;
P. Botella, J.M. López-Nieto, B. Solsona, A. Mifsud, F. Márquez, J. Catal. 209 (2002) 445;
P. Botella, J.M. López-Nieto, A. Dejoz, M.I. Vázquez, A. Martínez-Arias, Catal. Today 78 (2003) 507.
[3] H.H. Kung, Adv. Catal. 40 (1994) 1.
[4] D. Linke, D. Wolf, M. Baerns, S. Zeyß, U. Dingerdissen, L. Mleczko, Chem. Eng. Sci. 57 (2002) 39;
D. Linke, D. Wolf, M. Baerns, O. Timpoe, R. Schlögl, S. Zeyß, U. Dingerdissen, J. Catal. 205 (2002) 16.
[5] E.M. Thorsteinson, T.P. Wilson, F.G. Young, P.H. Kasai, J. Catal. 52 (1978) 116.
[6] H. Jiang, W. Lu, H. Wan, J. Mol. Catal. A 208 (2004) 213.
[7] K. Oshihara, T. Hisano, W. Ueda, Top. Catal. 15 (2001) 153.
[8] E.A. Mamedov, V. Cortés Corberán, Appl. Catal. A 127 (1995) 1.
[9] G. Mestl, J. Raman Spectrosc. 33 (2002) 333;
G. Mestl, J. Mol. Catal. A 158 (2000) 45.
[10] I.E. Wachs, Catal. Today 27 (1996) 437.
[11] M.A. Bañares, I.E. Wachs, J. Raman Spectrosc. 33 (2002) 259.
[12] I.E. Wachs, Personal communication.
[13] A. Neiman, S. Barsanov, J. Solid State Electrochem. 5 (2001) 382.
[14] H. Dai, A.T. Bell, E. Iglesia, J. Catal. 221 (2004) 491.
[15] K. Abraham, et al. JCPDS file #35-0334, $V_{0.87}Mo_{0.13}O_{2.17}$, J. Electrochem. Soc. 128 (1981) 2493.
[16] JCPDS file #21-0576, (Mo0.3V0.7)2O5, Kihlborg, Acta Chem. Scand., 21, 2495, 1967.
[17] JCPDS file #18-0850, MoV2O7.5, Freundlich, Pailleret, C.R. Seances Acad. Sci. (Paris), 261, 153, 1965.
[18] JCPDS file #18-0851, MoV2O8, Freundlich, Pailleret, C.R. Seances Acad. Sci. (Paris), 261, 153, 1965.
[19] Tudo et al., JCPDS file #18-0852, MoVO5, Tridot, C.R. Seances Acad. Sci. (Paris), 260, 3410, 1965.
[20] JCPDS file #20-1377, V2MoO8, Eick, Kihlborg, Acta Chem.Scand., 20, 1658, 1966.
[21] Freerka et al., JCPDS file #19-0812, Mo4V6O25, Dmuchovsky, J. Catal., 4, 291, 1965.
[22] Munch, R. Pierron, JCPDS file #34-0527, Mo6V9O40, J. Catal., 3, 406, 1964.
[23] Munch, R., Pierron, JCPDS, file #34-0530, Mo4V6O25, J. Catal., 3, 406, 1964.
[24] JCPDS file #18-1454, VOMoO4, Eick, Kihlborg, Acta Chem. Scand., 20, 722, 1966.
[25] JCPDS file #30-0849, Mo0.67V0.33O2, Marinder, B., Mater. Res. Bull., 10, 909, 1975.
[26] JCPDS file #31-1437, (V0.07Mo0.93)5O14, Ekstrom, Tilley, J. Solid State Chem., 19, 125, 1976.
[27] G. Mestl, T.K.K. Srinivasan, Catal. Rev. Sci. Eng. 40 (1998) 451.
[28] G. Mestl, Ch. Linsmeier, R. Gottschall, M. Dieterle, J. Find, D. Herein, J. Jäger, Y. Uchida, R. Schlögl, J. Mol. Catal. A 162 (2000) 463.
[29] M. Dieterle, G. Mestl, J. Jäger, Y. Uchida, H. Hibst, R. Schlögl, J. Mol. Catal. A 174 (2001) 169.
[30] I.E. Wachs, G. Deo, B.M. Weckhuysen, A. Andreini, M.A. Vuurman, M. de Boer, M.D. Amiridis, J. Catal. 161 (1996) 211.
[31] G. Plazenet, E. Payen, J. Lynch, B. Rebours, J. Phys. Chem. B 106 (2002) 7013.
[32] X. Carrier, J.-F. Lambert, M. Che, J. Am. Chem. Soc. 119 (1997) 10137.
[33] L. Le Bihan, P. Blanchard, M. Fournier, J. Grimblot, E. Payen, J. Chem. Soc., Faraday Trans. 94 (1998) 937.
[34] M.A. Bañares, M.V. Martínez-Huerta, X. Gao, I.E. Wachs, J.L.G. Fierro, Stud. Surf. Sci. Catal. A 130 (2000) 3125.
[35] X. Gao, M.A. Bañares, I.E. Wachs, J. Catal. 188 (1999) 325.
[36] G. García Cortez, M.A. Bañares, J. Catal. 209 (2002) 43.
[37] I.E. Wachs, J.-M. Jehng, G. Deo, B.M. Weckhuysen, V. Guliants, J.B. Bezinger, Catal. Today 32 (1996) 47.
[38] A. Magnéli, Acta Cryst. 6 (1953) 495.
[39] N.N. Greenwood, A. Earnshaw, Chemistry of the Elements, Pergamon Press, 1990.
[40] N.N. Greenwood, Ionic Crystals, Lattice Defects and Non-stoichiometry, Butterworths, London, 1968.
[41] M.O. Guerrero-Pérez, J. Al-Saeedi, V.V. Guliants, M.A. Bañares, Appl. Catal. A 260 (2004) 93.
[42] M. Kurzawa, G. Dabrowska, J. Thermal Anal. Calorim. 56 (1999) 217.
[43] M. Kurzawa, G. Dabrowska, J. Therm. Anal. Calorim. 60 (2000) 183.
[44] M. Kurzawa, G. Dabrowska, Solid State Ion. 101–103 (1997) 1189.
[45] A. Bielanski, M. Najbar, Appl. Catal. A 157 (1997) 223.
[46] M.O. Guerrero-Pérez, M.A. Bañares, Chem. Commun. (2002) 1292.
[47] B.M. Weckhuysen, Chem. Commun. (2002) 97.
[48] M.A. Bañares, M.O. Guerrero-Pérez, J.L.G. Fierro, G. García Cortéz, J. Mater. Chem. 12 (2002) 3337.
[49] M.A. Vuurman, D.J. Stufkens, A. Oskam, G. Deo, I.E. Wachs, J. Chem. Soc., Faraday Trans. 92 (1996) 3259.
[50] M.A. Vuurman, I.E. Wachs, J. Mol. Catal. 77 (1992) 29.
[51] C.T. Campbell, Surf. Sci. Rep. 27 (1997) 1.
[52] R. González Elipe, F. Yubero, Handbook of surfaces and interfaces of materials, in: H.S. Nalwa (Ed.), Surface and Interface Analysis and Properties, vol. 2, Academic Press, 2001, p. 147.
[53] M.A. Bañares, J.H. Cardoso, F. Agulló Rueda, J.M. Correa-Bueno, J.L.G. Fierro, Catal. Lett. 64 (2000) 191.
[54] B. Olthof, A. Khodakov, A.T. Bell, E. Iglesia, J. Phys. Chem. B 104 (2000) 1516.
[55] C.B. Wang, Y. Cai, I.E. Wachs, Langmuir 15 (1999) 1223.
[56] B. Pillep, P. Behrens, U.-A. Schubert, J. Spengler, H. Knözinger, J. Phys. Chem. B 103 (1999) 9595.
[57] M.O. Guerrero-Pérez, J.L.G. Fierro, M.A. Vicente, M.A. Bañares, J. Catal. 206 (2002) 339.